 CMES, vol.11, no.1, pp.37-48, 2006

The Bauschinger Effect's Impact on the 3-D Combined SIFs for Radially Cracked Fully or Partially Autofrettaged Thick-Walled Cylinders

M. Perl [1], **C. Levy** [2] **and V. Rallabhandy** [2]

Abstract: The Bauschinger Effect (BE) impact on K_{IN}– the combined, Mode I, 3-D Stress Intensity Factor (SIF) distributions for arrays of radial, internal, surface cracks emanating from the bore of a fully or partially autofrettaged thick-walled cylinder is investigated. A in-depth comparison between the combined SIFs for a "realistic" - Bauschinger Effect Dependent Autofrettage (BEDA) and those for an "ideal" - Bauschinger Effect Independent Autofrettage (BEIA) is performed. The 3-D finite element (FE) analysis is performed employing the submodeling technique and singular elements along the crack front. Both autofrettage residual stress fields, BEDA and BEIA, are simulated using an equivalent temperature field and more than 1200 different crack configurations are analyzed. SIFs for numerous crack arrays, **n**, a wide range of crack depth to wall thickness ratios, **a/t**, various ellipticities, **a/c**, several values of the yield-stress to pressure ratio, ψ, and different levels of autofrettage, ε, are evaluated. Autofrettage efficiency, η, for all BEDA cases is determined, and is compared with that of BEIA. The largest combined SIF K_{Nmax} is found to vary with angular location along the crack front and number of cracks and therefore needs to be evaluated for each particular case. The Bauschinger Effect is found to have a dramatic detrimental impact on the fatigue life of the thick-walled cylinder. For a partially autofrettaged thick-walled cylinder, $\varepsilon < 100\%$, it is found that the lower the level of autofrettage, the smaller the Bauschinger Effect is. Increasing ε beyond 60% is found to be counterproductive and is not recommended.

keyword: Bauschinger Effect, Autofrettage, Pressure Vessel.

1 Introduction

Autofrettage was introduced to thick-walled cylinders in the form of gun barrels almost a century ago (Kendall (2000)) in order to increase their operational pressure. Further on, it was realized that the favorable compressive residual stresses introduced by autofrettage was additionally beneficial by impeding, or at least delaying, crack initiation and by slowing down fatigue crack growth, thus extending the fatigue life of the cylinder. Such thick-walled cylinders are exposed to high pressure cyclic loading, acute temperature gradients and a corrosive environment during the firing process. As a result of these factors and the possible presence of stress concentrators such as gun rifling, numerous cracks develop at the inner surface of the cylinder. Experimental observations show that a large array of very similar semi-elliptical, radial, internal cracks may develop at the inner surface of the cylinder. In order to predict the cylinder's loading capacity and its fatigue life span, the effective three dimensional stress intensity factors (SIF) – K_{Ieff} that exists at the crack front of these cracks must be evaluated. In general, K_{Ieff} results from three different loads: $\boldsymbol{K}_{IP}$ - the stress intensity factor caused by pressure; $\boldsymbol{K}_{IA}$ - The negative SIF due to the compressive residual stresses introduced by autofrettage, negative in the context of superposition; and $\boldsymbol{K}_{IT}$ - the SIF resulting from the temperature field. In the case of a typical gun barrel, K_{IT} values are found to be in general negative and much smaller in absolute terms than those of K_{IP} and K_{IA} (for example, Perl and Greenberg, (1999)). Therefore, the analysis of barrels usually neglects K_{IT} and is based on $\boldsymbol{K}_{IN}$ - the combined SIF, $K_{IN} = K_{IP} - |K_{IA}|$.

The effectiveness of autofrettage in reducing the combined SIF K_{IN} is directly proportional to the magnitude of the residual compressive stresses from the cylinder's inner wall and throughout the inner portion of the cylinder wall. For any given geometry of the cylinder and overstressing process, the level of the residual compressive stresses and their distribution is highly dependent on

[1] University of Canterbury, Christchurch, NZ. On leave from the BenGurion University of the Negev, Beer Sheva, Israel
[2] Florida International University, Miami, FL , USA

the specific characteristics of the cylinder material. In a process that involves loading and unloading such as in both hydraulic and swage autofrettage processes, the material's behavior under such conditions actually determines the level of benefit that autofrettage can provide.

Hill (1950) suggested the first model for the evaluation of the autofrettage residual stress field. This analytical model includes both the elastic and the plastic deformation of the thick-walled cylinder assuming an elastic-perfectly-plastic material, von Mises yield criterion and incompressibility. Furthermore, it is assumes that the material has equal yield stress values in tension and in compression. Thus, unloading is completely elastic as long as the cylinder outer radius to inner radius ratio, R_o/R_i, is less than 2.22.

Bauschinger (1881) discovered the effect bearing his name, and found that cyclic change in loading conditions resulting in plastic deformation causes continuous change of the yield stress. A material subjected to a certain amount of plastic deformation in tension (or compression) subsequently undergoing reversed loading i.e., compression (tension), often exhibits a reduction in its yield stress. The ratio between the reduced yield stress and the initial one is usually termed the *Bauschinger Effect Factor* (BEF). Therefore, the Bauschinger Effect might impact the residual stress field introduced by autofrettage as the process involves a loading-unloading cycle with plastic deformation. Milligan, Koo and Davidson (1966) studied experimentally the BE in a modified 4330 high-strength steel used for gun barrels in the mid 1960's. Their major conclusion was that the BE increases with increasing permanent strain up to about 2%. Thereafter, the BEF tends to level off at a value of 0.35.

Others have attempted to incorporate the BE into autofrettage analysis, Chen (1986), Chaaban, Leung and Burns (1986), and Parker and Underwood (1998), among others. None of the models employed was able to simulate the complete nonlinearity of the unloading phase of autofrettage. In 1997, Jahed and Dubey suggested an improved algorithm that can account for the varying BEF within the re-yielding zone, which was further extended by Parker, Underwood and Kendall (1999). Its application by Parker and associates (1999, 2001) resulted in a more realistic evaluation of the autofrettage residual stress field.

Recently, a first attempt to determine the impact of the Bauschinger Effect on three-dimensional SIFs for internal radial cracks in a fully or partially autofrettaged gun barrel was made by Perl, Levy and Rallabhandy (2005). Stress intensity factors due to autofrettage for a large number of crack configurations were evaluated. K_{IA} values were obtained with and without the Bauschinger Effect. The Bauschinger Effect was found to reduce the beneficial stress intensity factor due to autofrettage, $K_{IA,}$ by up to 56%, as compared to the case of "ideal" autofrettage.

Based on the results previously obtained by the authors, it is the intention of the present analysis to:

a. Determine the distributions of the combined SIF, K_{IN}, along the crack front of numerous semi-elliptical crack configurations that may exist in a thick-walled cylinder with "realistic"- Bauschinger Effect Dependent Autofrettage (BEDA) and to compare the results with K_{IN} values for "ideal"-Bauschinger Effect Independent Autofrettage (BEIA), based on Hill's (1950) solution;

b. Determine the dependence of the favorable effect of autofrettage on $\psi = \sigma_{yp}/p$, the ratio of the internal pressure in the barrel, p, and the cylinder's material yield stress, σ_{yp}, for both BEDA and BEIA; and,

c. Determine the impact of the BE on the total fatigue life of the thick-walled cylinder.

2 Methodology

2.1 Simulation Of Autofrettage

The "ideal" plane-strain solution for a fully or partially autofrettaged thick-walled cylinder was derived by Hill (1950), assuming an elastic-perfectly-plastic material, using von Mises yield criterion and the incompressibility condition. The analysis yielded analytical expressions for the residual field stress components given by:

$$\sigma_{rr} = \begin{cases} \frac{\sigma_{yp}}{\sqrt{3}}\left[\left(2\ln\frac{r}{\rho} - 1 + \frac{\rho^2}{R_0^2}\right) - P_1\left(\frac{1}{R_0^2} - \frac{1}{r^2}\right)\right]; \\ \qquad\qquad R_i \le r \le \rho \\ \frac{\sigma_{yp}}{\sqrt{3}}\left(\rho^2 - P_1\right)\left(\frac{1}{R_0^2} - \frac{1}{r^2}\right); \\ \qquad\qquad \rho \le r \le R_0 \end{cases} \quad (1)$$

$$\sigma_{\theta\theta} = \begin{cases} \frac{\sigma_{yp}}{\sqrt{3}}\left[\left(2\ln\frac{r}{\rho} + 1 + \frac{\rho^2}{R_0^2}\right) - P_1\left(\frac{1}{R_0^2} + \frac{1}{r^2}\right)\right]; \\ \qquad\qquad R_i \le r \le \rho \\ \frac{\sigma_{yp}}{\sqrt{3}}\left(\rho^2 - P_1\right)\left(\frac{1}{R_0^2} + \frac{1}{r^2}\right); \\ \qquad\qquad \rho \le r \le R_0 \end{cases} \quad (2)$$

where r and θ are the radial and angular coordinates, σ_{yp} is the yield stress of the material, ρ is the radius of the

autofrettage interface, and P_1 is given by the expression:

$$P_1 = \frac{R_i^2 \cdot R_o^2}{R_0^2 - R_i^2}\left[1 - \frac{\rho^2}{R_0^2} + 2\ln\frac{\rho}{R_i}\right] \quad (3)$$

The "realistic" autofrettage used in this investigation was evaluated numerically by Parker (2001) extending Jahed and Dubey's (1997) procedure. Parker (2001) incorporated the Bauschinger Effect in the unloading phase with variable BEF based on Milligan, Koo and Davidson (1966), assumed Engineering Plane Strain conditions, i.e., constant axial strain with no net axial force, and used the von Mises yield criterion. Typical residual hoop stresses for various levels of "realistic" autofrettage (ε=10%-100%) for a cylinder of radii ratio of R_o/R_i=2 are given in Figure 8 of Parker, Underwood and Kendall (1999). An extensive comparison between the BEDA and BEIA autofrettage residual stress fields is given in Perl, Levy and Rallabhandy (2005).

The residual stress field pattern changes when cracking occurs at the inner surface of the cylinder. The evaluation of the redistribution of the residual stresses in this instance is not straightforward. A proper active thermal load can be used to create thermal stresses, identical to the autofrettage stress field, in the cylinder as well as to accurately reproduce the stress redistribution resulting from the development of cracks or notches in the cylinder (Pu and Hussain (1983)). Hence, such an equivalent thermal load was implemented in the Finite Element (FE) analysis used in this investigation.

The equivalent thermal load for Hill's (1950) autofrettage case was derived analytically by Parker and Farrow (1980), and is given by the following temperature field:

$$T(r) = \begin{cases} T_i - \frac{T_i - T_\rho}{\ln \rho/R_i}\ln\frac{r}{R_i}\ ; R_i \le r \le \rho \\ \\ T_\rho\ ;\ \rho \le r \le R_0 \end{cases} \quad (4)$$

where T_i is an arbitrary reference temperature usually chosen as nil, and the temperature gradient is given by:

$$T_i - T_\rho = \frac{2\sigma_{yp}}{\sqrt{3}} \cdot \frac{2(1-\upsilon)\ \ln\rho/R_i}{E\alpha} \quad (5)$$

where α is the linear coefficient of thermal expansion, E is the Young's modulus of elasticity and ν is the Poisson's ratio.

Parker's (2001) Bauschinger Effect Dependent Autofrettage (BEDA) field is given numerically in terms of the residual hoop stress values at discrete points throughout the cylinder's wall (see Fig. 8 in Parker (2001)). Perl (1988) provided an exact numerical algorithm that enables the direct evaluation of the equivalent temperature field for simulating any analytically or numerically expressed autofrettage residual stress field. In order to apply Perl's algorithm to Parker's BEDA, one needs to first evaluate the residual radial stress component, σ_{rr}, for Parker's solution,. This can be numerically extracted from equilibrium considerations. Once both $\sigma_{\theta\theta}^{BEDA}$ and σ_{rr}^{BEDA} are determined, the equivalent thermal load can be evaluated.

2.2 The Three-Dimensional Analysis

The three dimensional analysis is performed by the FE method. The cylinder is modeled as an elastic cylinder of inner radius, R_i, outer radius, R_o, wall thickness, t, ($R_o/R_i = 2, t = R_i$), and length 2L (see Fig. 1a). The cylinder contains n identical, evenly spaced, inner radial, semi-elliptical cracks of length, 2c and depth a. A segment of the cylinder showing two of the n cracks is presented in Fig. 1a. End effects are nullified by taking the ratio of the cylinder length to the crack as 2L/2c=10. The cartesian coordinates are X, Y and Z.

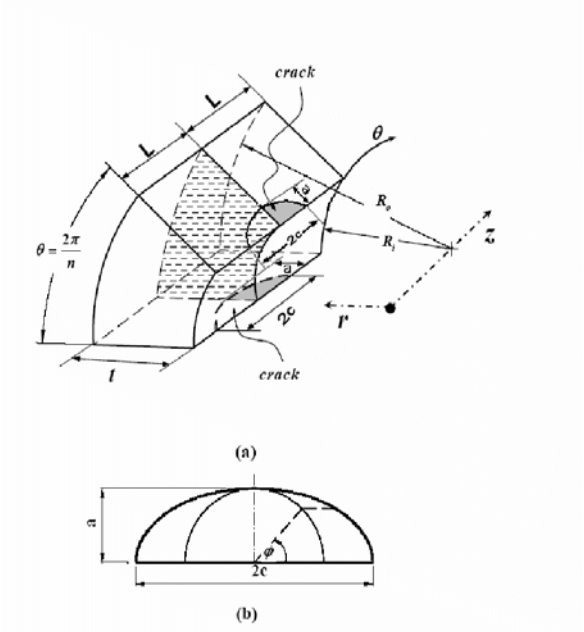

Figure 1 : (a) Cylinder segment employed in the FE model; (b) Definition of the angle ϕ for the SIF evaluation

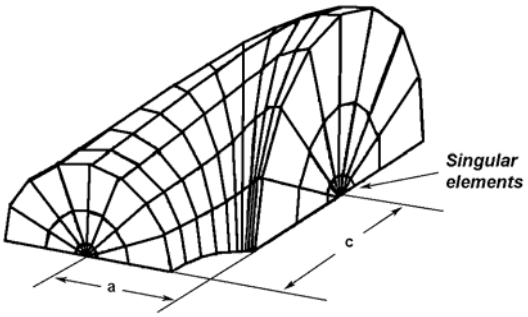

Figure 2 : The meshed submodel

2.3 Finite Element Idealization

Due to the various symmetries of the geometrical configuration, only part of the cylinder must be analyzed. The planes of symmetry, $Z = 0, \theta = 0^o$, $\theta = 2\pi/n^o$ (see Fig. 1a) allow us to model only that part of the cylinder enclosed within them. At Z=L the cylinder is assumed to be free of loads and unconstrained. As previously described, the autofrettage residual stress field for both BEDA and BEIA is simulated by the proper equivalent thermal load.

Though there were several elegant methods available to solve this problem (see, for example, Han and Atluri (2002), or So, Lau and Ng (2004)), the straightforward FEM method was chosen for its availability and simplicity. The model is solved using ANSYS, a standard FE code, in two consecutive steps via the submodeling technique. In the first step, a global mesh of the entire segment is generated using 10-node tetrahedron elements while applying a half automatic meshing procedure. The elements are varied in size, small near the crack front and gradually increased when moving away from it. The displacements obtained from the global mesh are used as boundary conditions for the submodel in the second stage.

In the second step, a toroidal submodel is created covering the crack front area with three layers of 20-node isoparametric elements (see Fig. 2). Elements collapsed to wedges form the singular elements at the crack front (Barsoum (1976)) for the first layer as well as two additional element layers above the first layer. The displacements from the global solution act as boundary conditions to the outer surface of the third layer. A comparison between the stress fields on the interface surface of the global and the submodels is performed to ensure a smooth transition between the two stages.

Convergence tests were performed using the stress intensity factor as the convergence criterion. Based on these trials, it is anticipated that the level of error will be less than 3% for meshes of more than 30,000 degrees of freedom (DOF). Hence, in order to maintain good accuracy while using reasonable computer resources, all meshes contained 30,000 to 40,000 DOF. The elements shape and aspect ratio for all meshes are automatically adjusted by the software.

SIFs are calculated from the submodel results using the code's crack-face displacement extrapolation procedure. The SIFs were calculated every 9 degrees from $\phi = 0^0$ to 90^0(see Fig. 1b). The results of the present model were validated against K_{IN}, K_{IP}, and K_{IA} values obtained by Perl and Nachum (2000, 2001) for "ideal" autofrettage, and against K_{IA} values obtained by Perl, Levy and Rallabhandy (2005) for "realistic" autofrettage. All the results were found to be in excellent agreement.

3 Results And Discussion

To study the impact of the Bauschinger Effect, as well as that of the different geometrical parameters on the combined stress intensity factor, K_{IN}, solutions for a large number of crack configurations are obtained. In order to maintain the same accuracy for K_{IP}, and K_{IA}, and thus for K_{IN}, K_{IP} and $K_{IA}$for each crack configuration are evaluated using the identical finite element breakdowns.

SIF distributions for radial semi-elliptical or semi-circular crack arrays are solved for the following set of parameters: n=1, 2,4, 8, 16, 32 and 64 cracks; crack ellipticities a/c = 0.5, 1 and 1.5; ratio of crack depth to wall thickness a/t=0.01,0.05, 0.1, 0.15 and 0.2 common in cylinders, with autofrettage levels of ε = 100%, 60%, and 30%.

To allow for the comparison of K_{IN} results for BEDA with existing results for BEIA (Perl and Nachum (2001)), as well as to readily be able to combine them with those of K_{IP}, all SIF values are normalized with respect to:

$$K_0 = \frac{pR_i}{t}\sqrt{\frac{\pi a}{Q}} \tag{6}$$

where pR_i/t represents the average circumferential stress in the cylinder, and Q is the shape factor for an elliptical crack. Q, which represents the square of a complete elliptic integral of the second kind, is usually approximated

by:

$$Q = 1 + 1.464\left(\frac{a}{c}\right)^{1.65} \quad for \quad a/c \le 1$$
$$Q = 1 + 1.464\left(\frac{c}{a}\right)^{1.65} \quad for \quad a/c \ge 1 \tag{7}$$

The favorable effect of autofrettage, for both BEDA and BEIA depends on the ratio, $\psi = \sigma_{yp}/p$. In the present analysis σ_{yp} is chosen to be 1172 MPa (170 ksi), representing the yield stress of a typical gun barrel steel. The values of ψ are chosen to be 1.93, 2.31, 2.89, and 3.55, where the first and last values represent the ratios for pressures of thick-walled cylinders used in modern tank barrels and classical tank barrels, respectively. The results are presented separately for a fully and a partially autofrettaged, thick-walled cylinder.

3.1 The Fully Autofrettaged Cylinder

K_{IN} results for the full autofrettage case, i.e., ε=100% are divided into three groups: semi-circular (a/c=1), slender semi-elliptical ($a/c < 1$), and transverse semi-elliptical ($a/c > 1$) cracks.

3.1.1 Semi-circular cracks

The combined SIF due to Bauschinger Effect Dependent Autofrettage along the crack front of a semi-circular surface crack for $\psi = \sigma_{yp}/p$=1.93, is presented in Fig. 3. In this figure, K_{IN}/K_0 *is* given as a function of ϕ for a crack of relative depth of a/t=0.05, for various crack arrays and is displayed in solid lines. For comparison purposes, K_{IN}/K_0 values due to Bauschinger Effect Independent Autofrettage for identical crack configurations, obtained by Perl and Nachum (2001), are also presented in this figure as solitary data points.

In all these crack configurations K_{IN}/K_0 distributions for both BEIA and BEDA follow a similar pattern, i.e., the maximum SIF, K_{Nmax}, occurs at $\phi = 0^o$ at the bore of the cylinder, decreasing almost monotonically with ϕ. While K_{IP} and K_{IA} usually reach their maximum absolute values for an array of two cracks (n=2), the largest combined SIF K_{Nmax} is attained, in this case, for n = 16. As the number of cracks in the array further increases, K_{Nmax} decreases.

Though similar in pattern, K_{IN}/K_0 values for BEDA are much higher than those for BEIA, i.e., K_{Nmax}(BEDA)/K_{Nmax}(BEIA) = 1.43, for n=2, to 1.68, for n=64. This 17% difference is attributable to the fact that

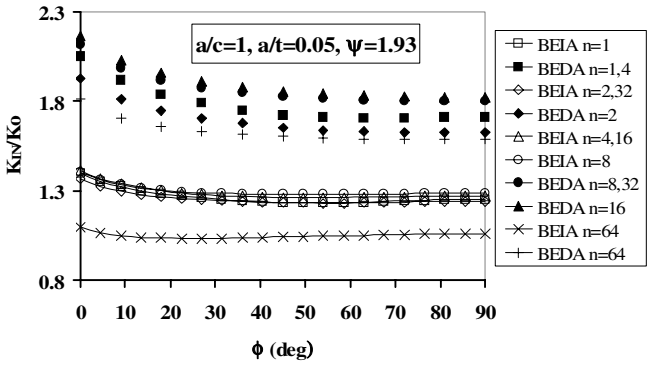

Figure 3 : K_{IN}/K_O variation along the crack front of semi-circular radial cracks in a fully autofrettaged thick-walled cylinder (a/t=0.05, ψ=1.93)

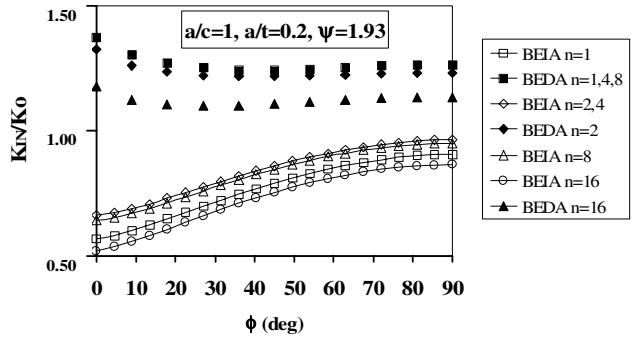

Figure 4 : K_{IN}/K_0 variation along the crack front of semi-circular radial cracks in a fully autofrettaged thick-walled cylinder (a/t=0.2, ψ=1.93)

K_{IA} due to BEDA is much smaller (in absolute value) than the one due to BEIA, contributing much less to the reduction of the combined SIF.

The results for a deeper semi-circular crack of depth a/t=0.2, is presented in Fig. 4. Unlike the case of the shallower crack, a/t=0.05 (see Fig. 3), K_{IN}/K_0 distributions for BEIA and BEDA follow a different pattern. In the BEDA case the combined SIF reaches its maximum at $\phi = 0^o$ and decreases monotonically with ϕ, whereas, in the BEIA case K_{IN}/K_0 increases monotonically with ϕ, reaching its maximum at $\phi = 90^o$ The largest SIF K_{max} is attained, for both BEIA and BEDA

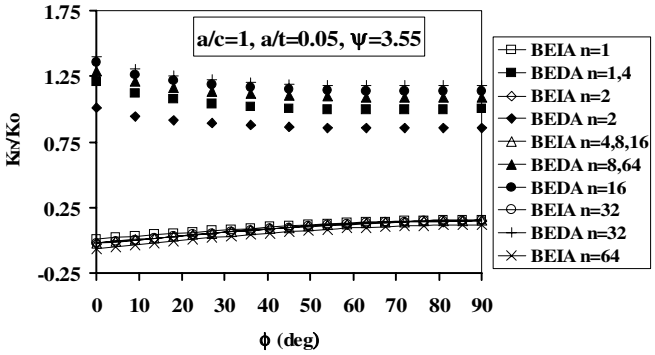

Figure 5 : K_{IN}/K_0 variation along the crack front of semi-circular radial cracks in a fully autofrettaged thick-walled cylinder (a/t=0.05, ψ=3.55)

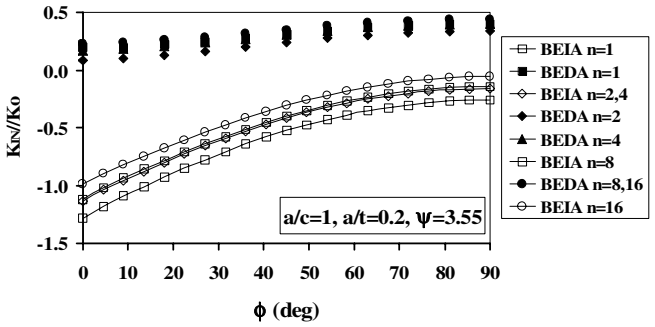

Figure 6 : K_{IN}/K_0 variation along the crack front of semi-circular radial cracks in a fully autofrettaged thick-walled cylinder (a/t=0.2, ψ=3.55)

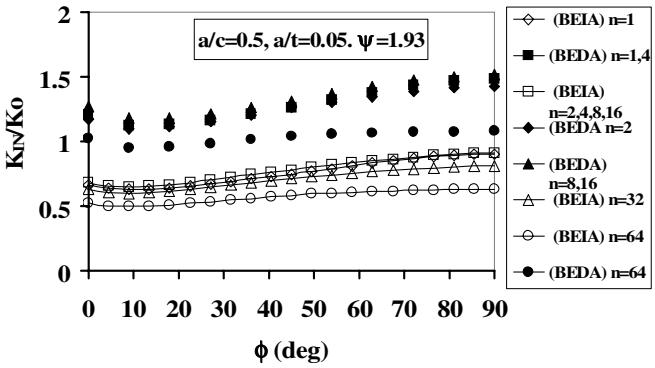

Figure 7 : K_{IN}/K_0 variation along the crack front of slender semi-elliptical radial cracks in a fully autofrettaged thick-walled cylinder (a/t=0.05, ψ=1.93)

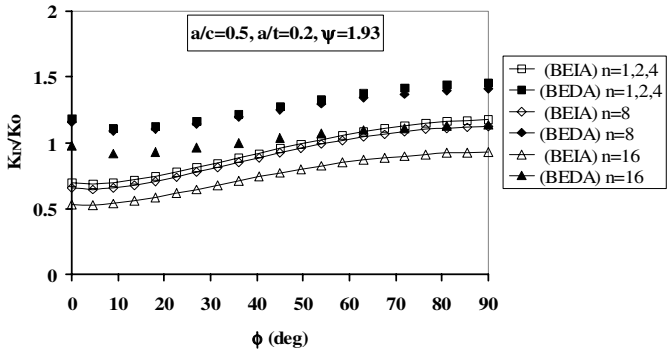

Figure 8 : K_{IN}/K_0 variation along the crack front of slender semi-elliptical radial cracks in a fully autofrettaged thick-walled cylinder (a/t=0.2, ψ=1.93)

for an array of n = 4 cracks, as compared to n=16 cracks in the previous case. As in the previous case, K_{IN}/K_0 values for BEDA are much higher than those for BEIA. K_{Nmax}(BEDA)/K_{Nmax}(BEIA) varies between 1.36, for n=16, to 1.52, for n=1.

It is important to note that in these two semi-circular crack configurations K_{IN} is always positive, i.e., the effect of the internal pressure is greater than that of autofrettage. However, this is a direct result of the particular ψ value chosen. For higher values of ψ, namely, lower pressures, p the favorable effect of autofrettage may overcome the effect of pressure, even yielding "negative" K_{IN} values. As previously explained, this means the crack is fully or a partially closed with a nil combined SIF along the closed portion of the crack. Figures 5 and 6 represent K_{IN}/K_0 for the same crack configurations as in Figs. 3 and 4, but for a ψ=3.55 (p= 3260 atm). In the case of the shallower crack, a/t=0.05 (see Fig. 5), the crack is always open for BEDA. However for BEIA, it is fully open only for n=1, while for denser crack arrays n=2-64, the crack is partially closed in the vicinity of the cylinder's inner wall ($\phi = 0^o - 20^o$). In the case of the deeper crack, in the BEDA case the crack is always open, $K_{IN}/K_0 > 0$, whereas for BEIA it is always fully closed, K_{IN}/K_0=0.

3.1.2 Slender semi-elliptical cracks

In Figs. 7 and 8, the combined SIF due to BEDA as a function of ϕ along the crack front of two slender semi-

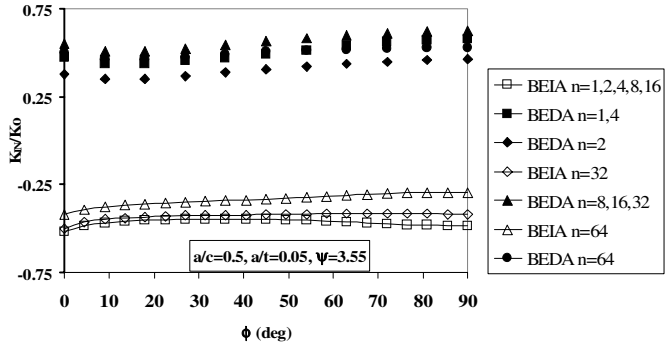

Figure 9 : K_{IN}/K_0 variation along the crack front of slender semi-elliptical radial cracks in a fully autofrettaged thick-walled cylinder (a/t=0.05, ψ=3.55)

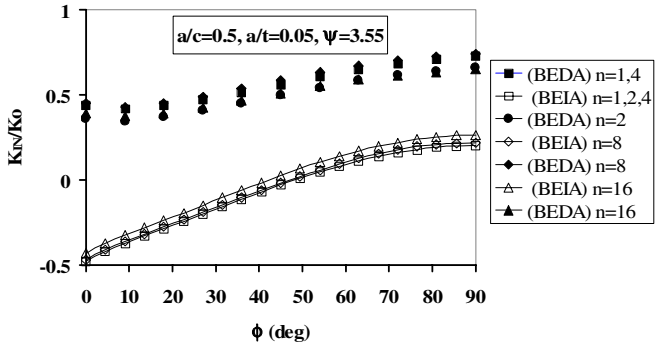

Figure 10 : K_{IN}/K_0 variation along the crack front of slender semi-elliptical radial cracks in a fully autofrettaged thick-walled cylinder (a/t=0.2, ψ=3.55)

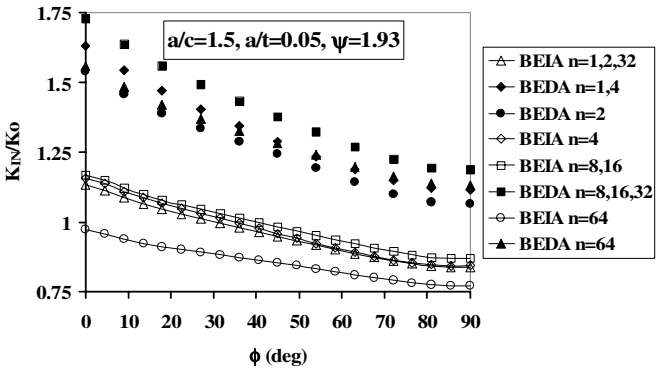

Figure 11 : K_{IN}/K_0 variation along the crack front of transverse semi-elliptical radial cracks in a fully autofrettaged thick-walled cylinder (a/t=0.05, ψ=1.93)

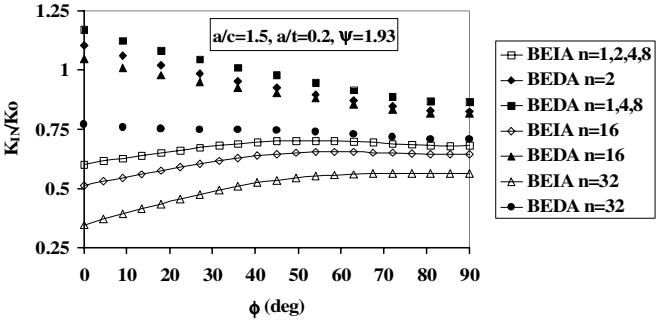

Figure 12 : K_{IN}/K_0 variation along the crack front of transverse semi-elliptical radial cracks in a fully autofrettaged thick-walled cylinder (a/t=0.2, ψ=1.93)

elliptical cracks (a/c=0.5) of relative depths of a/t=0.05, and 0.2, for ψ=1.93, are presented. K_{IN}/K_0 values due to BEIA for identical crack configurations, obtained by Perl and Nachum (2001), are also presented.

K_{IN}/K_0 distributions have a common pattern for both BEIA and BEDA for the above crack configurations, namely, reaching the maximum combined SIF value, K_{Nmax}, at $\phi = 90^o$ In the BEDA case, the largest K_{Nmax} occurs for an array of n=16 shallow cracks (a/t=0.05) and for an array of n=4 deeper cracks (a/t=0.2), while in the BEIA case, the largest K_{Nmax} is achieved for an array of two cracks (n=2).

For the semi-elliptical slender cracks, K_{IN}/K_0 values for BEDA are much higher than those for BEIA, as in the case of semi-circular cracks. K_{Nmax}(BEDA)/K_{Nmax}(BEIA) for the shallower crack, a/t=0.05, varies between 1.57, for n=2, to 1.70, for n=64, while for the deeper crack length, a/t = 0.2, the ratio is about 1.23, practically independent of n.

As a result of the relative high pressure case, namely when ψ=1.93, K_{IN} is always positive for the examples presented in Figs. 7 and 8. For the same crack configurations, once a more moderate relative pressure is chosen, e.g., ψ=3.55, the situation completely changes as can be seen from Figs. 9 and 10. In the BEDA case, K_{IN}/K_0 is always positive for both crack depths. However, in the BEIA case, while the deeper crack, a/t=0.2 is still partially open (e.g., for n=16 and $\phi > 40^o$), the shallower crack, a/t=0.05, is always closed and K_{IN}/K_0 =0.

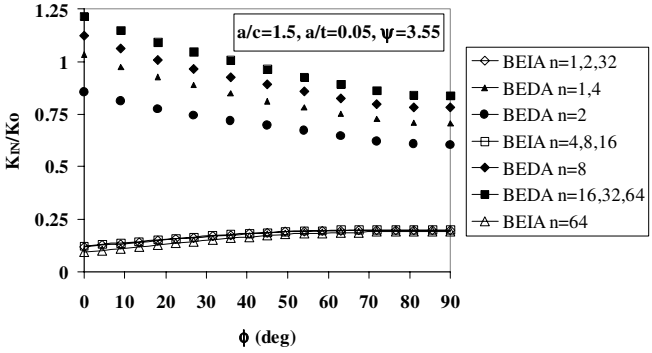

Figure 13 : K_{IN}/K_0 variation along the crack front of transverse semi-elliptical radial cracks in a fully autofrettaged thick-walled cylinder (a/t=0.05, ψ=3.55)

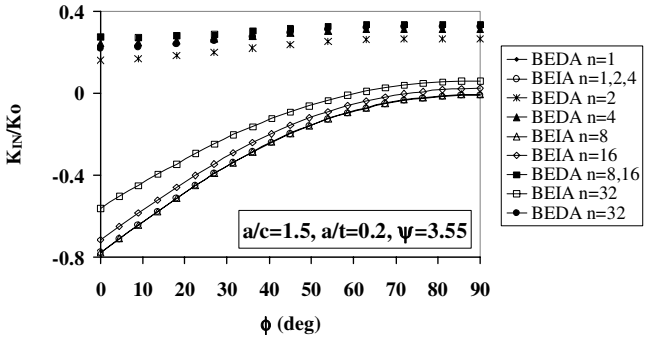

Figure 14 : K_{IN}/K_0 variation along the crack front of transverse semi-elliptical radial cracks in a fully autofrettaged thick-walled cylinder (a/t=0.2, ψ=3.55)

3.1.3 Transverse semi-elliptical cracks

Given in Figures 11 and 12 are the distribution of the combined SIF due to BEDA and for comparison those of BEIA (from Perl and Nachum (2001)), as a function of ϕ along the crack front of two transverse semi-elliptical cracks (a/c=1.5) of relative depths of a/t=0.05, and 0.2, for ψ=1.93.

The patterns of all curves are reminiscent of those found in the semi-circular case (see Figs. 3 and 4). For the shallow cracks, a/t=0.05, K_{Nmax} occurs at $\phi = 0^o$ for an array of n=16 cracks for both BEIA and BEDA. For the deeper crack BEIA and BEDA follow different patterns. Whereas K_{Nmax} occurs at $\phi = 0^o$ for n=1 in the BEDA case, the maximum in the BEIA case shifts to $\phi = 54^o$ for an array of n=4 cracks.

In the transverse semi-elliptical case, as in the semi-circular and the slender semi-elliptical cases, K_{IN}/K_0 valuesfor BEDA are much larger than those for BEIA. K_{Nmax}(BEDA)/K_{Nmax}(BEIA) for the shallower crack, a/t=0.05, varies between 1.35, for n=2, to 1.60, for n=64, while for the deeper crack length, a/t=0.2, the ratio varies between 1.69, for n=1, to 1.37, for n=32.

The combined SIF is positive for all the cases in Figs. 11 and 12 in the relative high pressure case, ψ=1.93. Once the pressure is decreased, ψ=3.55, the results for the same crack configurations change dramatically, as reflected in Figs. 13 and 14. In the BEDA case, K_{IN}/K_0 is always positive for both crack depths. However, in the BEIA case, while the shallow crack, a/t=0.05 is completely open, the deeper cracks, a/t=0.2, are mostly closed except for n=16, $\phi > 77^o$, and n=32, $\phi > 63^o$.

3.2 The Efficiency of Autofrettage

The magnitude of the combined SIF, K_{IN}, is highly dependent on the impact of autofrettage, which in turn depends on the yield-stress to pressure ratio $\psi = \sigma_{yp}$/p, as well as on the susceptibility of the cylinder's material to the Bauschinger Effect. In order to quantitatively analyze the efficiency of autofrettage, an efficiency factor, η, is defined:

$$\eta = (1 - K_{Nmax}/K_{Pmax}) * 100\% \tag{8}$$

Here, η represents the relative reduction (in percent) in the maximal combined SIF, K_{Nmax}, due to the presence of autofrettage (K_{IA}), as compared to the case of "no autofrettage" when only K_{Pmax} prevails. The higher the value of η, the higher the impact of autofrettage, i.e., η=100% represent a "closed crack" with K_{Nmax}=0.

Substituting the definition of K_{Nmax} into Eq. 8 and rearranging:

$$\eta = [1 - (K_{IP}/K_{Pmax} - |K_{IA}|/K_{Pmax})_{max}] * 100\% \tag{9}$$

In Eq. 9, for any given location of K_{Nmax} along the crack front, the first term in the parenthesis is independent of both p and σ_{yp}, while the second term is linear in ψ. Therefore, as long as $\eta < 100\%$ and for a fixed location of K_{Nmax}, η is a linear function of ψ for both BEIA and BEDA. If in a certain case the K_{Nmax} location changes

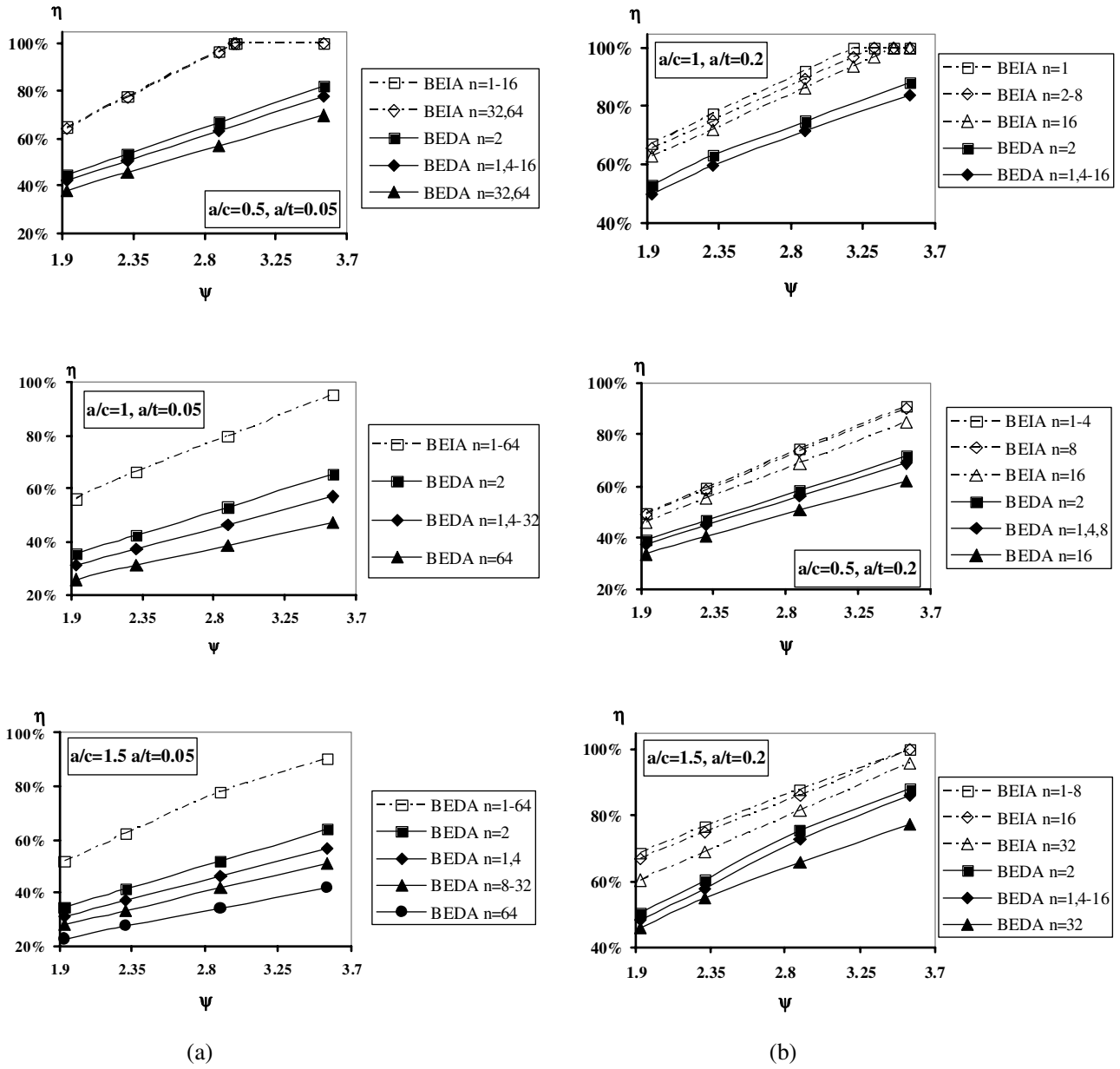

Figure 15 : (a) η as a function of ψ for all BEDA and BEIA cases (a/t=0.05); (b) η as a function of ψ for all BEDA and BEIA cases (a/t=0.2)

with ψ, some slight nonlinearity in η vs. ψ right occur. In the following, the parameter η is analyzed for BEIA and BEDA separately.

3.2.1 Bauschinger Effect Independent Autofrettage

Figures 15 present η as a function ψ for all the BEIA and BEDA cases previously discussed. It is clear that as ψ increases, the relative influence of autofrettage increases, and, thus, its efficiency η increases, as could have been expected. When ψ=1.93, η is in the range of 46% to 69%, while for ψ=2.31, 2.89, and 3.55, η values are in the range of 55% to 77%, 69% to 97%, and 85% to 100%, respectively.

For the shallower cracks, a/t=0.05, η is essentially independent of the number of cracks in the array, n, and as the crack ellipticity increases, η *decreases*. In contrast, for the case of the deeper cracks, a/t=0.2, η *increases* with

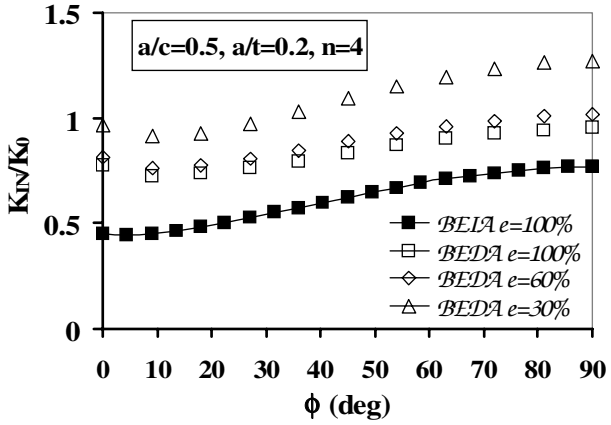

Figure 16 : K_{IN}/K_0 variation along the crack front of four slender radial cracks in a fully and partially autofrettaged thick-walled cylinder (a/c=0.5, a/t=0.2, ψ=1.93)

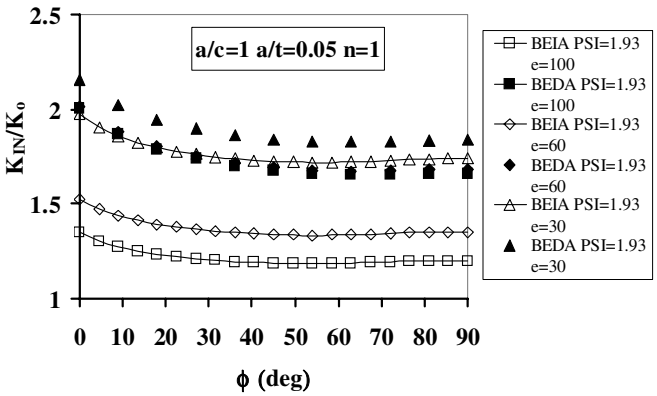

Figure 17 : K_{IN}/K_0 variation along the crack front of semi-circular radial cracks in a fully and partially autofrettaged thick-walled cylinder (a/t=0.05, ψ=1.93)

ellipticity, but decreases slightly as n becomes larger.

3.2.2 Bauschinger Effect Dependent Autofrettage

When the cylinder's material is susceptible to the Bauschinger Effect, the impact of autofrettage might lessen considerably (see Perl, Levy and Rallabhandy (2005)). This of course is reflected in a general decrease in η as reflected in BEDA curves of Figs. 15. In the BEDA, as in the BEIA, the higher ψ is, the higher η becomes (see Eq. 9). For ψ=1.93, η is in the range of 23% to 53%, while for ψ=2.31, 2.89, and η values are in the range of 27% to 63%, 34% to 76%, and 42% to 88%, respectively. All these values are much lower than their counterparts in the BEIA case.

In all the BEDA cases, η is maximal for an array of n=2 cracks, decreasing monotonically as n becomes larger, irrespective of the value of ψ. The influence of ellipticity differs between deep and shallow cracks. In the case of deep cracks, η is maximal in the semi-circular case. For shallow cracks, η decreases as a/c increases.

3.3 The Partially Autofrettaged Cylinder

In many practical situations, cylinders, such as gun barrels, may be partially autofrettaged as was discussed in Perl, Levy and Rallabhandy (2005). K_{IN} is evaluated for all crack configurations and for both BEIA and BEDA for various levels of autofrettage, i.e., ε = 30%, 60%, 100%. Typical results are shown in Figs. 16 and 17. Figure 16 shows the combined SIF distributions for four slender cracks of depth a/t=0.2, whereas Fig. 17 shows the combined SIF distribution for one (n=1) semi-circular crack of relative depth a/t=0.05, resulting from various autofrettage levels for both BEIA and BEDA, and with ψ=1.93.

In the BEIA case for Fig. 17, the largest combined SIFs for the three levels of autofrettage, ε=100%, 60%, and 30%, are K_{Nmax}/K_0 =1.350, 1.525, and 1.974 respectively, whereas in the BEDA case K_{Nmax}/K_0 =2.001, 2.016, and 2.157, respectively. By reducing the level of autofrettage for BEIA from 100% to 30%, the maximal combined SIF is increased by a level of 13% for ε =60%, and by more than 46% for ε=30%. In the BEDA case the increase in K_{Nmax}/K_0 is less than 1% for ε =60%, and less than 8% for ε=30%. This emphasizes the fact that the lower the level of autofrettage, the smaller the BE is. For higher values of ψ, the positive impact of autofrettage is larger; thus, this effect is more pronounced.

Actually, for BEDA, the difference between the largest combined SIF for ε=100% and ε =60% is very small, and is in the range of 0.7% for ψ=1.93 and 2.3% for ψ=3.55. By increasing the level of autofrettage from ε=60% to ε=100%, a very small beneficial effect is gained in marginally reducing K_{Nmax}. But this increase is offset by increasing the tensile stress at the outer diameter, resulting in a higher susceptibility to cracking from the cylinder's outer surface.

4 Concluding Remarks

The impact of the Bauschinger Effect (BE) on the three-dimensional, Mode I, combined SIF, $K_{IN,}$ distributions as well as on its maximal value K_{Nmax}, for arrays of radial, internal, surface cracks emanating from the bore of a fully or partially autofrettaged, thick-walled cylinder were investigated. More than 1200 cases were solved and the effect of five parameters (the number of cracks in the array, n; crack ellipticity, a/c; crack depth, a/t; the ratio $\psi = \sigma_{yp}$/p; and the BEDA level, ε) were extensively examined and thoroughly compared with the results for BEIA.

The cylinder's loading capacity and its fatigue life depend on the maximal SIF K_{Nmax}. The magnitude of K_{Nmax} and its location along the crack front vary from case to case. For example, for a crack of depth a/t=0.2 in a cylinder with ψ=1.93 and BEDA, the largest K_{Nmax} occurs at $\phi = 90^o$ in an array of n=4 cracks for a slender semi-elliptical crack (a/c=0.5), occurs at $\phi = 0^o$ for an array of n=4 semi-circular cracks (a/c=1.0), and occurs at $\phi = 0^o$ for one transverse semi-elliptical crack (a/c=1.5). For the same a/t and ψ case but for BEIA, the largest K_{Nmax} will occur: for a slender semi-elliptical crack (a/c=0.5) in an array of n=2 cracks at $\phi = 90^o$, for a semi-circular crack (a/c=1.0) in an array of n=4 cracks at $\phi = 90^o$, and for a transverse semi-elliptical crack (a/c=1.5) in an array of n=4 cracks at $\phi = 54^o$. Thus, K_{Nmax} can be located at any angular location along the crack front and can reach its largest values for arrays of any number of cracks from 1 to 16, and, therefore, needs to be evaluated for each particular case.

The magnitude of the maximal combined SIF, $K_{Nmax,}$ is determined by the cylinder's material susceptibility to the Bauschinger Effect and by the yield stress-to-pressure ratio $\psi = \sigma_{yp}$/p, as previously explained. As an example of the impact BE might have on the fatigue life of the cylinder, ψ=1.93 is assumed, where autofrettage's beneficial effect is minimal. Here, the ratio between K_{Nmax}(BEDA)/K_{Nmax}(BEIA) varies between 1.21 (for a/t=0.2, a/c=0.5, and n=2) to 1.70 (for a/t=0.05, a/c=0.5, and n=64). As a first crude approximation, if a Paris exponent of n_P=3.0 is assumed, typical of thick-walled cylinder material used in gun barrels, the ratio of the fatigue lives would be N_f(BEDA) / N_f(BEIA) = 0.2-0.56, namely, BE might reduce the total fatigue life by a factor of about 2 to 5. For larger values of ψ this factor can reach values of more than 100, and, in certain cases, when autofrettage completely dominates the pressure, a theoretically infinite fatigue life is predicted for BEIA versus a finite fatigue life for BEDA. The detrimental influence of the Bauschinger Effect becomes more pronounced for shallow cracks as the number of cracks in the array and crack ellipticity increase and as ψ decreases. For deeper cracks, the damaging influence of the BE : 1) is relatively much smaller; 2) is slightly dependent on n; 3) decreases as ψ increases; and, 4) is minimal for semi-circular cracks.

For a partially autofrettaged thick-walled cylinder, it was found that the lower the level of autofrettage, the smaller the impact of the Bauschinger Effect. The influence of the Bauschinger Effect is even smaller for higher values of ψ for which the positive impact of autofrettage is larger. Increasing the level of autofrettage beyond ε=60% is found to have only a marginal positive impact in reducing the critical combined SIF, but results in a higher susceptibility to cracking from the cylinder's outer surface. This suggests that thick-walled cylinders should not be autofrettaged to levels beyond ε=60% if no other process is applied to them.

References

Barsoum, R. S. (1976): On the use of isoparametric finite elements in linear fracture mechanics. *Int. J. Num. Meth. in Eng.*, vol. 10, pp. 25- 37.

Bauschinger, J. (1881): Uber die veranderung der elasticitätsgrenze und des elasticitätsmoduls verschiedener metalle. *Zivilingenieur*, vol. 27, columns 289-348.

Chaaban, A.; Leung, K.; Burns, D. J. (1986): Residual stresses in autofrettaged thick-walled high pressure vessels. *ASME PVP* vol. 110, pp. 55-60.

Chen, P. C. T. (1986): Bauschinger and hardening effects on residual stresses in autofrettaged thick-walled cylinders. *Trans. ASME, J. Pressure Vessel Tech.*, vol. 108, pp. 108-112.

Han, Z. D.; Atluri, S. N. (2002): SGBEM (for cracked local subdomain)—FEM (for uncracked global structure) alternating method for analyzing 3D surface cracks and their fatigue-growth. *CMES: Computer Modeling in Engineering & Sciences*, vol. 3, pp. 699-716.

Hill, R. (1950): *The mathematical theory of plasticity*, Clarendon Press, Oxford.

Jahed, H.; Dubey, R. N. (1997): An axisymetric method for elastic-plastic analysis capable of predicting residual stress field. *Trans. ASME, J. Pressure Vessel Tech.*, vol. 119, pp. 264-273.

Kendall, D. P. (2000): A short history of high pressure technology from Bridgeman to Division 3. *Trans. ASME, J. Pressure Vessel Tech.*, vol. 122, pp. 229-233.

Milligan, R. V.; Koo, W. H.; Davidson, T. E. (1966): The Bauschinger effect in a high strength steel. *Trans. ASME, J. Basic Eng.*, vol. 88, pp. 480-488.

Parker, A. P.; Farrow, J. R. (1980): On the Equivalence of Axisymetric bending, thermal, and autofrettage residual stress fields. *J. Strain Anal.*, vol. 15, pp. 51-52.

Parker , A. P.; Underwood, J. H. (1998): Influence of the Bauschinger effect on residual stresses and fatigue lifetimes in autofrettaged thick-walled cylinders. *Fatigue and Fracture Mechanics, 29th Vol. ASTM STP 1321*. T. L. Panontin and S. D. Sheppard, eds., ASTM, PA.

Parker, A. P.; Underwood, J. H.; and Kendall, D. P. (1999): Bauschinger effect design procedure for autofrettaged tubes including material removal and Sachs' method. *Trans. ASME, J. Pressure Vessel Tech*, vol. 121, pp. 430-437.

Parker, A. P. (2001): Autofrettage of open-end tubes – pressure, stresses, strains, and code comparison. *Trans. ASME, J. Pressure Vessel Tech.*, vol. 123, pp. 271-281.

Perl, M. (1988): The temperature field for simulating partial autofrettage in an elasto-plasic thick-walled cylinder. *Trans. ASME, J. Pressure Vessel Tech.*, vol. 110, pp. 100-102.

Perl, M.; Greenberg, Y. (1999): Three dimensional analysis of thermal shock effect on inner semi-elliptical surface cracks in a cylindrical pressure vessel. *Int. J. Fracture*, vol. 99, pp. 163-172.

Perl, M.; Nachum A. (2000): 3-D stress intensity factors for internal cracks in an over-strained cylindrical pressure vessel, part I - the effect of autofrettage level. *Trans. ASME, J. Pressure Vessel Tech.*, vol. 122, pp. 421-426.

Perl, M.; Nachum A. (2001): 3-D Stress intensity factors for internal cracks in an over-strained cylindrical pressure vessel, part II - the combined effect of pressure and autofrettage. *Trans. ASME, J. Pressure Vessel Tech.*, vol. 123, pp. 135-138.

Perl, M.; Levy, C.; Rallabhandy, V. (2006): The influence of the bauschinger effect on 3-D stress intensity factors for internal radial cracks in a fully or partially autofrettaged gun barrel. *Accepted, Trans. ASME, J. Pressure Vessel Tech*.

Pu, S. L.; Hussain, M. A. (1983): Stress intensity factors for radial cracks in a partially autofrettaged thick-walled cylinder. *Fracture Mechanics: Fourteen Symposium-Vol. I: Theory and Analysis*, eds. J. C. Lewis and G. Sines, ASTM-STP 791, pp. I-194- I-215.

So, W. M. G.; Lau, K. J.; Ng, S. W. (2004): Determination of stress intensity factors for interfacial cracks using the virtual crack extension approach. *CMES: Computer Modeling in Engineering & Sciences*, vol. 5, pp. 189-200.